

# Adaptive Control for Spacecraft Formation Flying with Solar Radiation Pressure and Reduction of Secular Drift

Aniketh Kalur,<sup>1</sup> Kavyashree Shivakumar,<sup>2</sup> Matthias Schmid,<sup>3</sup> and John L. Crassidis<sup>4</sup>

**Abstract**—A major problem faced while trajectory planning of spacecraft formation flying is obtaining a “drift-free” case to optimize fuel consumption. The paper considers the effect of non-linearity on relative motion dynamics of spacecraft formation flying with disturbance caused by solar radiation pressure on the formation of spacecraft. The non-linearity is a function of initial conditions, and a perturbation approach is used to correct the initial conditions while maintaining the formation in bounds and also satisfying the zero secular growth requirements. A full state feedback adaptive control law is developed which accounts for the solar radiation pressure, and also estimates and updates the unknown spacecraft mass for formation keeping. The relative dynamics are written as a function of the true anomaly ensuring that the control law works effectively for highly eccentric orbits. Lastly, a Lyapunov stability analysis is shown to ensure the stability of the controller.

## I. INTRODUCTION

Coordination of satellites in formation flying helps distribute the mission task among many satellites. The use of satellites in formation helps in better coverage of the Earth, increase in resolution of science data, provides faster ground track repeats, and also helps to increase redundancy. Distributed spacecraft performing space-based sensing, imaging, and communication provide large aperture areas at the cost of maintaining a meaningful formation geometry with minimal error. Further, by allowing instruments on separate spacecraft to be combined into a co-observatory, formation flying can replace an expensive multiple-payload platform with a large number of low-cost spacecraft [1].

A conceptual difference between formation flying problems that result in two or more vehicles docking and spacecraft formation flying of maintaining a relative orbit of a cluster is that the latter is significantly more sensitive to relative orbit modeling errors [2]. From a controls perspective a rendezvous problem requires less precision as the feedback laws are robust for minor errors made in the modeling. The same is not true for the case of formation flying of spacecraft that have to maintain a relative orbit for their

lifetime. Maintaining the relative formation in presence of unknown, time varying disruptive disturbances has proven to be a challenging problem for control engineers.

The Clohessy-Wiltshire (CW) equations model the relative motion dynamics between the follower and leader spacecraft, under the assumptions of a circular reference orbit, spherical Earth and linearized differential equations [3]. The existing literature on the study of relative motion dynamics of satellites proves that there exists two types of perturbations: intrinsic and exogenous disturbances. Intrinsic disturbances arise due to the non-linearity of the differential gravitational acceleration, eccentricity of the reference and the Earth’s oblateness. These three are the most important perturbations that breakdown the circular orbit solutions to the CW equations [3], while the external disturbances can be due to various factors such as atmospheric drag, solar radiation pressure, J2 perturbations, etc.

Solar Radiation Pressure (SRP) is a non conservative force acting on a spacecraft. Among all non-gravitational forces SRP is the largest, and hence can have a significant influence on orbital dynamics. In this paper we use the SRP force model that has been used for most analytical studies. The force caused by SRP acts along the object-Sun line, directly away from the Sun. The model of SRP pressure used in this paper is commonly referred to as the “cannonball” model, and the mathematical model will be discussed in section II-B. The assumption is made that the spacecraft is in High Earth Orbit (HEO); this enables us to neglect the shadow regions and the effect of atmospheric drag as well.

In this paper, the problem of satellite formation flying with disturbances arising due to SRP is considered. The nonlinear version of the CW equations are used to design a learning controller. This controller adapts to the disturbances entering the system model. Another important aspect addressed is accounting for the nonlinear and eccentric perturbations to obtain bounded relative orbits. The process of changing the CW initial conditions to eliminate secular growth and obtaining bounded relative orbits [3] has also been used.

## II. MODEL

### A. Relative Dynamics

The relative nonlinear dynamics of the follower is given by the CW equations as [2]

<sup>1</sup> Graduate Student, Mechanical and Aerospace Department, University at Buffalo, The State University of New York, Amherst, NY 14260-4400 [anikethk@buffalo.edu](mailto:anikethk@buffalo.edu)

<sup>2</sup> Graduate Student, Mechanical and Aerospace Department, University at Buffalo, The State University of New York, Amherst, NY 14260-4400 [kbukkamb@buffalo.edu](mailto:kbukkamb@buffalo.edu)

<sup>3</sup> Ph.D. Candidate, Mechanical and Aerospace Department, University at Buffalo, The State University of New York, Amherst, NY 14260-4400 [mjschmid@buffalo.edu](mailto:mjschmid@buffalo.edu)

<sup>4</sup> CUBRC Professor in Space Situational Awareness, Mechanical and Aerospace Department, University at Buffalo, The State University of New York, Amherst, NY 14260-4400 [johnnc@buffalo.edu](mailto:johnnc@buffalo.edu)

$$\begin{aligned}
\ddot{x} - 2\dot{\theta}\dot{y} - \ddot{\theta}y - \dot{\theta}^2x + \frac{\mu(r_l+x)}{[(r_l+x)^2+y^2+z^2]^{\frac{3}{2}}} - \frac{\mu}{r_l^2} &= 0 \\
\ddot{y} + 2\dot{\theta}\dot{x} - \ddot{\theta}x - \dot{\theta}^2y + \frac{\mu y}{[(r_l+x)^2+y^2+z^2]^{\frac{3}{2}}} &= 0 \quad (1) \\
\ddot{z} + \frac{\mu z}{[(r_l+x)^2+y^2+z^2]^{\frac{3}{2}}} &= 0
\end{aligned}$$

where  $x$ ,  $y$  and  $z$  are the relative position of follower with respect to leader in local-vertical-local-horizontal (LVLH) coordinate system,  $\mu$  is the gravitational parameter,  $\theta$  is time varying true anomaly of the leader spacecraft,  $\dot{\theta}$  is the rotational velocity of the reference frame, and  $r_l$  is the instantaneous distance of leader spacecraft from the Earth, given by

$$r_l = \frac{a(1-e^2)}{1+e\cos\theta(t)} \quad (2)$$

where  $a$  is the semi-major axis of the leader and  $e$  is the eccentricity of the leader.

The relative dynamics are written as a function of the true anomaly ensuring that the control law works effectively for highly eccentric orbits. Hence  $\theta(t)$  and  $\dot{\theta}(t)$  are given by

$$\begin{aligned}
\dot{\theta}(t) &= \frac{n}{(1-e^2)^{3/2}} [1+e\cos\theta(t)]^2 \\
\ddot{\theta}(t) &= -2n^2 \sin\theta(t) \left[ \frac{1+e\cos\theta(t)}{1-e^2} \right]^3
\end{aligned}$$

where  $n = \sqrt{\mu/a^3}$  is the mean motion of the leader. Pre-multiplying (1) with the mass of the follower,  $m_f$ , the nonlinear dynamics of follower can be regrouped in the form given by

$$m_f \ddot{\mathbf{q}}_f + C(\dot{\theta}) \dot{\mathbf{q}}_f + D(\ddot{\theta}, \dot{\theta}, r_f) \mathbf{q}_f + N_l = 0 \quad (3)$$

where  $\mathbf{q}_f = [x \ y \ z]^T$  and  $r_f = [(r_l+x)^2+y^2+z^2]^{\frac{1}{2}}$ . The matrix  $C$  is a skew-symmetric Coriolis-like matrix given by

$$\begin{aligned}
C(\dot{\theta}) &= 2\dot{\theta}m_f \begin{bmatrix} 0 & -1 & 0 \\ 1 & 0 & 0 \\ 0 & 0 & 0 \end{bmatrix}, \\
D(\ddot{\theta}, \dot{\theta}, r_f) &= m_f \begin{bmatrix} \frac{\mu}{r_f^3} - \dot{\theta}^2 & -\ddot{\theta} & 0 \\ \ddot{\theta} & \frac{\mu}{r_f^3} - \dot{\theta}^2 & 0 \\ 0 & 0 & \frac{\mu}{r_f^3} \end{bmatrix}
\end{aligned}$$

Also,  $N_l$  is a nonlinear term defined as

$$N_l = m_f \left[ \frac{\mu r_l}{r_f^3} - \frac{\mu}{r_l^2}, \quad 0, \quad 0 \right]^T$$

Using method of virtual work for the insertion of differential force due to solar radiation pressure, control inputs for the leader and the follower spacecraft, the nonlinear relative position dynamics of the follower is

$$m_f \ddot{\mathbf{q}}_f + C(\dot{\theta}) \dot{\mathbf{q}}_f + D(\ddot{\theta}, \dot{\theta}, r_f) \mathbf{q}_f + N_l + \mathbf{f}_u(u_l) + \mathbf{F}_{SRP} = \mathbf{u}_f \quad (4)$$

where

$$\mathbf{f}_u(u_l) = \frac{m_f}{m_l} [u_{lx} \ u_{ly} \ u_{lz}]^T, \quad \mathbf{u}_f = [u_{fx} \ u_{fy} \ u_{fz}]^T$$

and  $\mathbf{F}_{SRP}$  is the difference between the force due to SRP on the follower and leader, given by

$$\mathbf{F}_{SRP} = m_f \Delta \mathbf{a}_{SRP} \quad (5)$$

### B. SRP Model

The model used for simulation of the SRP disturbance force is given by the cannonball model as [4]

$$\mathbf{f}_{SRP} = -P_{\odot} C_{SRP} S \hat{\mathbf{u}}_{SAT} \quad (6)$$

where  $P_{\odot}$  is the pressure of solar radiation,  $C_{SRP}$  is the coefficient of reflectivity,  $S$  is the surface area of the spacecraft perpendicular to the Sun, and  $\hat{\mathbf{u}}_{SAT}$  is the unit position vector from the satellite to the center of the Sun. The disturbance acceleration [5] acting on a spacecraft can be characterized as

$$\mathbf{a}_{SRP} = -\sigma \frac{S}{m} \hat{\mathbf{u}}_{SUN}$$

where  $m$  is the mass of the spacecraft and  $\sigma$  is a constant that includes the effect of the distance to the Sun and reflectivity of the spacecraft. In our case we take  $\sigma = 7 \times 10^{-6}$ . For the purpose of simplification the distance between the spacecraft and Earth is neglected, hence  $\hat{\mathbf{u}}_{SUN}$  is a unit vector pointing to the Earth from the Sun. As mentioned in section I the shadow region has been neglected for HEO applications.

The variable  $\Delta \mathbf{a}_{SRP}$  is used for the difference in SRP forces between the leader and follower spacecraft in LVLH frame:

$$\Delta \mathbf{a}_{SRP} = -\sigma \Delta \frac{S}{m} \hat{\mathbf{u}}_{SUN|LVLH} \quad (7)$$

where  $\hat{\mathbf{u}}_{SUN|LVLH}$  is the unit vector from the Sun pointing to the Earth in the LVLH frame.

**Remark 1:** The left hand side of (4) produces an affine parameterization [6]:

$$m_f \ddot{\boldsymbol{\xi}} + C \dot{\mathbf{q}}_f + D \mathbf{q}_f + N_l + \mathbf{f}_u(u_l) = Y(\boldsymbol{\xi}, \dot{\mathbf{q}}_f, \mathbf{q}_f, \ddot{\theta}, \dot{\theta}, r_l, r_f, \mathbf{u}_l) \boldsymbol{\phi} \quad (8)$$

where  $\boldsymbol{\xi} = [\xi_x, \xi_y, \xi_z]^T$  is a dummy variable. The matrix  $Y$  is a regression matrix given by

$$Y = \begin{bmatrix} \xi_x - 2\dot{\theta}\dot{y} - \ddot{\theta}y - \dot{\theta}^2x + \frac{\mu(r_l+x)}{r_f^3} - \frac{\mu}{r_l^2} & u_{lx} \\ \xi_y + 2\dot{\theta}\dot{x} - \ddot{\theta}x - \dot{\theta}^2y + \frac{\mu y}{r_f^3} & u_{ly} \\ \xi_z + \frac{\mu z}{r_f^3} & u_{lz} \end{bmatrix}$$

and  $\boldsymbol{\phi}$  is an unknown constant system parameter consisting of the mass of the spacecraft:

$$\boldsymbol{\phi} = \left[ m_f \quad \frac{m_f}{m_l} \right]^T$$

**Remark 2:** Parameterization of perturbation force is considered by combining the force and acceleration equations, given by (5) and (7), of the SRP respectively, as

$$\mathbf{F}_{SRP} = A_k \mathbf{f}_d(t) \quad (9)$$

where  $A_k = m_f \Delta_m^{\frac{s}{m}}$  is the unknown constant disturbance parameter. The term  $\Delta_m^{\frac{s}{m}}$  has a very small value and hence can be neglected over an orbit; this therefore lets us make the previously mentioned assumption. Also,  $\mathbf{f}_d(t) = -\sigma \hat{\mathbf{u}}_{SUN|LVLH}$  is a function of time that depends on the unit vector pointing to the Earth from the Sun.

### III. ADAPTIVE LEARNING CONTROL LAW

In this section, a control law is formulated such that the relative position of follower,  $\mathbf{q}_f$ , tracks a desired relative trajectory  $\mathbf{q}_{df}(t)$ , i.e.

$$\lim_{t \rightarrow \infty} \mathbf{q}_f(t) = \mathbf{q}_{df}(t)$$

The adaptive control law for the model in (4) is developed such that the tracking error,  $\mathbf{e}$ , exhibits asymptotic stability. For the purpose of designing a controller, a combined error [7] variable  $\boldsymbol{\eta}(t) \in \mathbb{R}^3$  is defined:

$$\boldsymbol{\eta} = \dot{\mathbf{e}} + \lambda_0 \mathbf{e} = \Delta(s) \mathbf{e} \quad (10)$$

where  $\lambda_0$  is an unknown constant, diagonal and positive definite matrix, and  $\Delta(s) = s + \lambda_0$  is a stable (Hurwitz) polynomial with Laplace variable  $s$ . The variable  $\boldsymbol{\eta}$  can be rewritten as

$$\boldsymbol{\eta} = \dot{\mathbf{q}}_f - \dot{\mathbf{q}}_r$$

where  $\dot{\mathbf{q}}_r$  is defined as

$$\dot{\mathbf{q}}_r = \dot{\mathbf{q}}_{df} - \lambda_0 \mathbf{e}$$

The control law can be designed as

$$\mathbf{u}_f = Y_r \hat{\boldsymbol{\phi}} - k \boldsymbol{\eta} + \hat{A}_k \mathbf{f}_d(t) \quad (11)$$

where  $k$  is a constant, positive definite matrix, and  $Y_r = Y(\ddot{\mathbf{q}}_{df} - \lambda_0 \dot{\mathbf{e}}, \dot{\mathbf{q}}_f, \mathbf{q}_f, \ddot{\theta}, \dot{\theta}, \theta, r_l, r_f, \mathbf{u}_l)$ . Using the above control law, the closed loop tracking error is given by

$$\dot{\boldsymbol{\eta}} \boldsymbol{\phi} + k \boldsymbol{\eta} = Y_r \tilde{\boldsymbol{\phi}} + \tilde{A}_k \mathbf{f}_d(t) \quad (12)$$

where

$$\tilde{\boldsymbol{\phi}} = \hat{\boldsymbol{\phi}} - \boldsymbol{\phi} \quad (13)$$

$$\tilde{A}_k = \hat{A}_k - A_k \quad (14)$$

Using the Laplace transformation, this can be rewritten as

$$\boldsymbol{\eta} = \frac{1/\boldsymbol{\phi}}{s + (k/\boldsymbol{\phi})} [Y_r \tilde{\boldsymbol{\phi}} + \tilde{A}_k \mathbf{f}_d(t)] \quad (15)$$

The above equation is of the form of Lemma 8.1 in pg. 324 of [7], where  $\frac{1/\boldsymbol{\phi}}{s + (k/\boldsymbol{\phi})}$  is a SPR transfer function. Using the aforementioned Lemma 8.1, the adaptation law can be designed as

$$\dot{\hat{\boldsymbol{\phi}}} = -\gamma Y_r' \boldsymbol{\eta} \quad (16)$$

$$\dot{\hat{A}}_k = -a_l \mathbf{f}_d(t)' \boldsymbol{\eta} \quad (17)$$

where  $\gamma$  is a constant, diagonal and positive definite matrix, and  $a_l$  is a positive constant.

In addition, the time derivatives of (13) and (14) are given by

$$\begin{aligned} \dot{\tilde{\boldsymbol{\phi}}} &\triangleq \dot{\hat{\boldsymbol{\phi}}} - \dot{\boldsymbol{\phi}} \\ \dot{\tilde{A}}_k &\triangleq \dot{\hat{A}}_k - \dot{A}_k \end{aligned} \quad (18)$$

Since the parameters  $\boldsymbol{\phi}$  and  $A_k$  are unknown constants, from (18) the parameter estimation error is given by:

$$\begin{aligned} \dot{\tilde{\boldsymbol{\phi}}} &\triangleq \dot{\hat{\boldsymbol{\phi}}} \\ \dot{\tilde{A}}_k &\triangleq \dot{\hat{A}}_k \end{aligned} \quad (19)$$

#### A. Stability Analysis

In this section a stability analysis on the controller is performed. The following non-negative candidate Lyapunov function is considered

$$V(t) = m_f \boldsymbol{\eta}^T \boldsymbol{\eta} + \gamma^{-1} \tilde{\boldsymbol{\phi}}^T \tilde{\boldsymbol{\phi}} + a_l^{-1} \tilde{A}_k^2 \quad (20)$$

Taking the time derivative of the above mentioned function along the closed-loop dynamics of (12) results in

$$\dot{V}(t) = 2m_f \boldsymbol{\eta}^T \dot{\boldsymbol{\eta}} + 2\gamma^{-1} \tilde{\boldsymbol{\phi}}^T \dot{\tilde{\boldsymbol{\phi}}} + 2a_l^{-1} \tilde{A}_k \dot{\tilde{A}}_k \quad (21)$$

It is straightforward to verify that

$$\dot{V} = -2|k| \boldsymbol{\eta}^T \boldsymbol{\eta} \quad (22)$$

As seen from (20) and (21),  $V$  is a positive definite function and  $\dot{V}$  is a negative semi-definite function. Hence,  $V$  is a non-increasing function, that implies  $V(t) \in L_\infty$ . All signals in closed loop system can be shown to remain bounded by utilizing the standard signal chasing arguments, employing the boundedness of all signals in closed-loop system and (12), we can conclude that  $\dot{\boldsymbol{\eta}}(t) \in L_\infty$ . Solving the differential (22), we get

$$V(0) - V(\infty) = 2|k| \int_0^\infty \|\boldsymbol{\eta}(t)\|^2 dt \quad (23)$$

Considering (23) and boundedness of  $V(t)$ , we can conclude that  $\dot{\boldsymbol{\eta}}(t) \in L_2, t \geq 0$ .

Using Barbalat's Lemma, we can conclude that  $\boldsymbol{\eta}(t)$  converges asymptotically, given by

$$\lim_{t \rightarrow \infty} \boldsymbol{\eta}(t) = 0 \quad (24)$$

Using the definition of  $\boldsymbol{\eta}(t)$  as in (10), the property  $\boldsymbol{\eta}(t) \in L_\infty \cap L_2$  and (24); Lemma 1.6 of [8] enables us to conclude that the adaptive learning control law ensures asymptotic convergence of the position and velocity tracking errors, given by

$$\lim_{t \rightarrow \infty} \mathbf{e}(t), \dot{\mathbf{e}}(t) = 0 \quad (25)$$

#### IV. REDUCTION OF SECULAR GROWTH

The intrinsic effects of nonlinearity and eccentricity in the dynamics of the relative motion breaks down the solution for the CW equations. In [4] a solution has been developed to help eliminate the secular growth in the CW equations. This is done by modifying the initial conditions for the follower spacecraft. A Taylor series expansion of the relative circular orbit gives

$$\begin{aligned}\ddot{x} - 2n\dot{y} - n^2x &= \frac{3\mu}{a^4} \left[ \frac{y^2 + z^2 - 2x^2}{2} \right] \\ \ddot{y} + 2n\dot{x} &= \frac{-3\mu}{a^4} xy \\ \ddot{z} + n^2z &= \frac{-3\mu}{a^4} xz\end{aligned}\quad (26)$$

This is the perturbed CW equation due to nonlinearity with  $\varepsilon = \frac{3\mu}{a^4}$  as the perturbation parameter. The solution to (26) is given by [4]

$$\begin{aligned}x &= x_h + \varepsilon x_{cn}, \quad \dot{x} = \dot{x}_h + \dot{x}_{cn}, \quad \ddot{x} = \ddot{x}_h + \ddot{x}_{cn} \\ y &= y_h + \varepsilon y_{cn}, \quad \dot{y} = \dot{y}_h + \dot{y}_{cn}, \quad \ddot{y} = \ddot{y}_h + \ddot{y}_{cn} \\ z &= z_h + \varepsilon z_{cn}, \quad \dot{z} = \dot{z}_h + \dot{z}_{cn}, \quad \ddot{z} = \ddot{z}_h + \ddot{z}_{cn}\end{aligned}\quad (27)$$

The subscript  $h$  refers to the solution to the CW equations and the subscript  $cn$  refers to the solution to the nonlinearity correction. The desired initial conditions are given by

$$\begin{aligned}\mathbf{X}_h(0) &= \begin{bmatrix} \frac{\rho}{2} \sin(\alpha_0) & \rho \cos(\alpha_0) & \rho \sin(\alpha_0) & \frac{\rho}{2} n \cos(\alpha_0) \\ & -\rho n \sin(\alpha_0) & \rho n \cos(\alpha_0) & 0 \end{bmatrix}^T \\ \mathbf{X}_{cn}(0) &= \begin{bmatrix} 0 & 0 & 0 & 0 \\ & \frac{-\rho}{48n} (12 + 6 \cos 2\alpha_0) & 0 & 0 \end{bmatrix}^T\end{aligned}\quad (28)$$

Similarly, the initial conditions for minimizing the effect of eccentricity is given by [4]. The required initial condition is

$$\dot{y}_0 = -\rho \sin \alpha_0 + \delta(e) \quad (29)$$

where the solution for  $\delta(e)$  is given by [4]

$$\delta(e) = n\rho \sin \alpha_0 \left[ 1 - \frac{2+e}{2(1+e)^{1/2}(1-e)^{3/2}} \right] \quad (30)$$

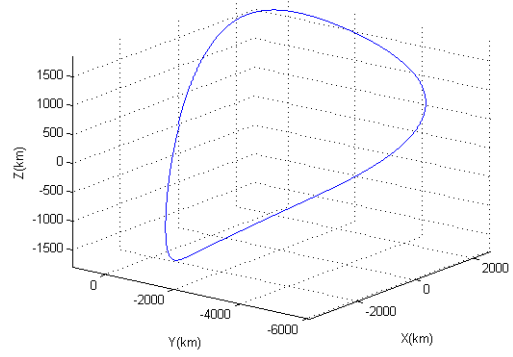
The initial conditions for balancing the combined effects of nonlinearity and eccentricity are made to the  $\dot{y}(0)$  term. Hence the initial condition for reduced secular growth is given by

$$\dot{y}(0) = -\rho \sin \alpha_0 + \delta(e) + \varepsilon \dot{y}_{cn}(0) \quad (31)$$

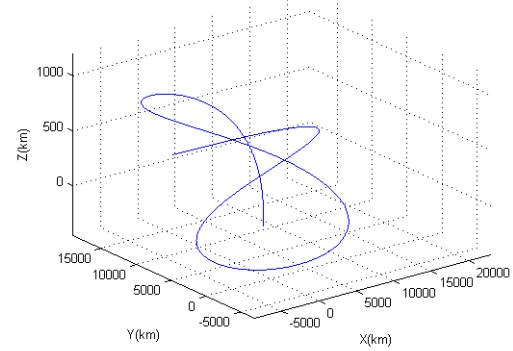
These initial conditions will be used to reduce the secular growth and minimize fuel consumption.

#### V. RESULTS

From the following simulations the effectiveness of the controller can be seen. Fig. 1b shows how that the effect of SRP causes the spacecraft to deviate from the reference orbit (Fig. 1a). In high eccentric orbits the effect can be seen more evidently as the SRP is dominant. This is undesirable to any engineer or person associated with the mission, as it



(a) Follower Trajectory Relative to the Leader



(b) Follower Trajectory Relative to the Leader with Effects of SRP without a Controller

Fig. 1: Relative Motion Trajectory

is clearly visible that any mission cannot be accomplished without a controller that will continuously work to keep the spacecraft in the desired orbit. It can be seen from Fig. 2 that the controller designed here is working to adapt itself to the disturbances and helps maintain the satellite in desired orbit.

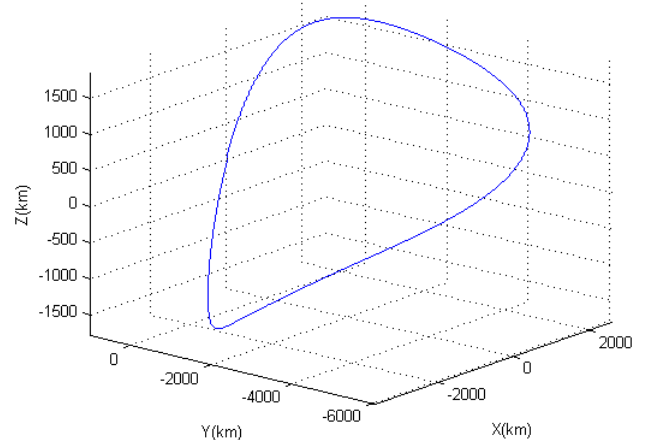


Fig. 2: Follower Trajectory Relative to the Leader with Controller and Disturbance

For the purpose of illustration and a numerical example,

TABLE I: Orbital Parameters

| $a$         | $e$      | $i$        | $\Omega$  | $\omega$  | $\theta(0)$ | $T$           | $\rho$     |
|-------------|----------|------------|-----------|-----------|-------------|---------------|------------|
| 42095<br>km | 0.818181 | $10^\circ$ | $0^\circ$ | $0^\circ$ | $180^\circ$ | 23.8756<br>hr | 1000<br>km |

TABLE II: Additional Parameters

| $m_l$   | $m_f$   | $u_l$         |
|---------|---------|---------------|
| 1250 Kg | 1250 Kg | $[0, 0, 0]^T$ |

data from the Magnetospheric Multiscale Mission (MMS) [9] is used. Actual orbital elements obtained from the mission specifications of MMS are used for propagation. The adaptive control described in (11) is simulated for the relative dynamics of the follower with respect to the leader spacecraft. The mission parameters used for the purpose of simulation are given in the Table I.

The relative trajectory of follower and leader spacecraft are numerically solved by using the thrust free dynamics given by (1). The initial conditions for the initial position are given by (31). The additional parameters used for the purpose of simulation are given in Table II.

The gains for the control law, i.e. learning, control and adaption gains mentioned previously are obtained through trial and error, which are shown in Table III. The actual trajectory for  $q_f$  is given by Fig. 1a. The trajectory with disturbance and without a controller can be seen in Fig. 1b. Fig. 2 shows the trajectory after using the controller to compensate for the disturbance. The errors and convergence of the estimates are shown in Fig. 3 and Fig. 4. It is seen that the errors are of the order  $10^{-4}$ ,  $10^{-7}$  and  $10^{-7}$  km along  $x$ ,  $y$  and  $z$  axis, respectively; this error is considered to be minimal in our controller. It is also seen that the estimates converge very well to their respected actual values.

TABLE III: Control Parameters

| $\lambda_0$      | $k$                            | $\gamma$              | $a_l$ |
|------------------|--------------------------------|-----------------------|-------|
| $I_{3 \times 3}$ | $3 \times 10^3 I_{3 \times 3}$ | $10^2 I_{2 \times 2}$ | 1000  |

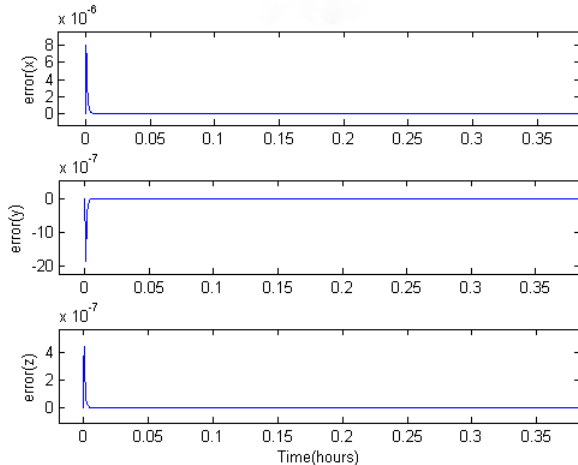


Fig. 3: Error Along the X, Y and Z Axes

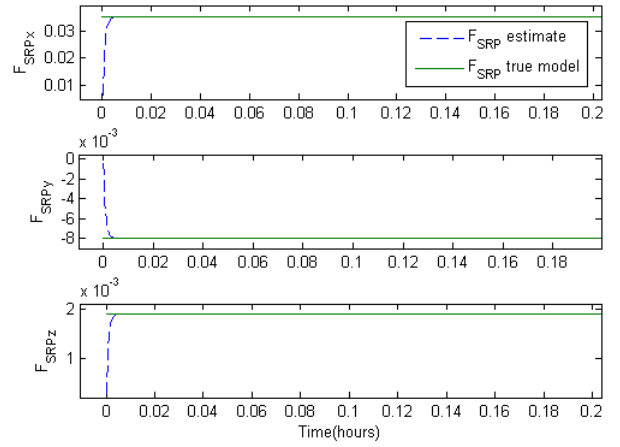
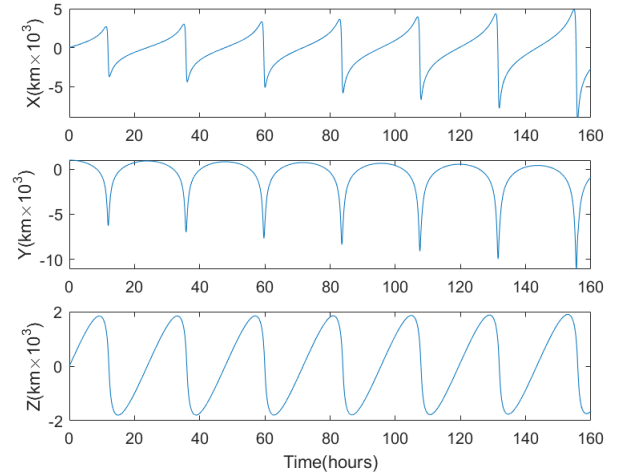
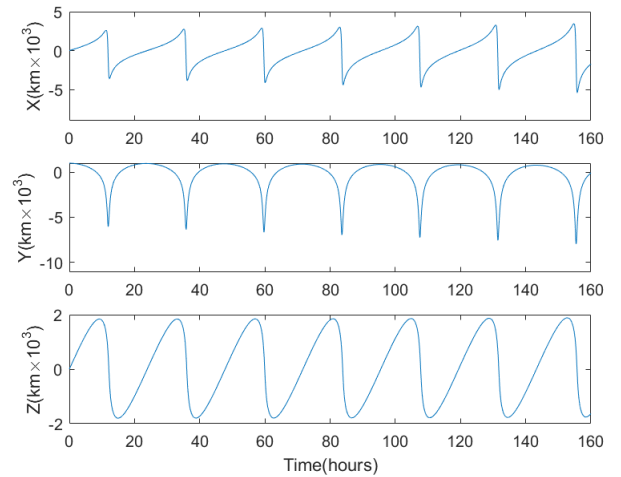


Fig. 4: Convergence of Estimated Value and Actual Value of  $F_{SRP}$



(a) Nonlinear Dynamics Simulation with Uncorrected Initial Conditions

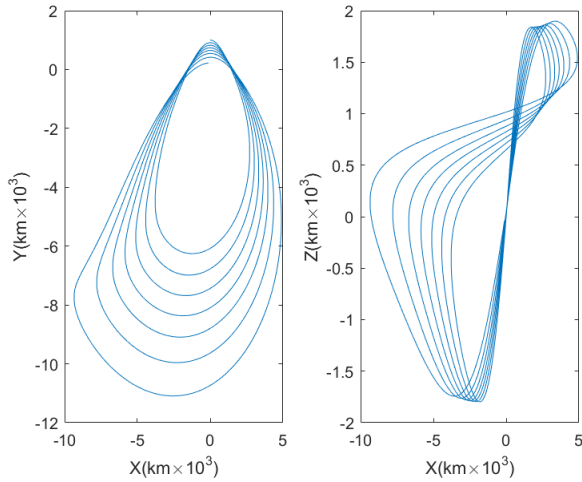


(b) Nonlinear Dynamics Simulation with Corrected Initial Conditions

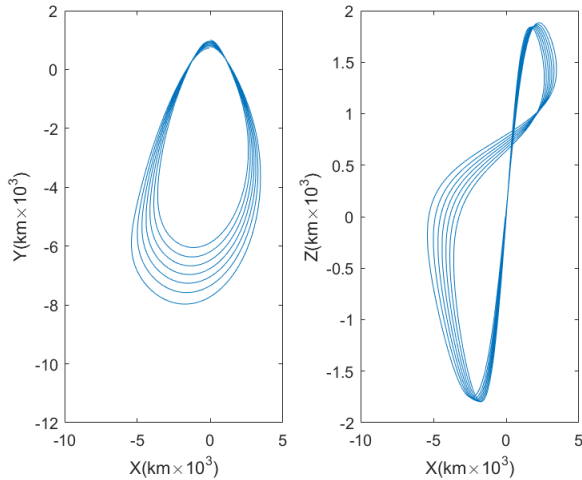
Fig. 5: Effect of Initial Conditions

The reduction of secular growth by correcting the initial

conditions can be seen in Fig. 5b and the uncorrected CW conditions are shown in Fig. 5a. Lastly the effect of secular growth on the complete orbits can be seen in Figs. 6a and 6b. Here it is clearly visible that changing the initial conditions has a great effect on the orbits over a prolonged time.



(a) Relative Orbit with Uncorrected Initial Conditions



(b) Relative Orbit with Corrected Initial Conditions

Fig. 6: Effect of Initial Conditions on Full Orbit

## VI. CONCLUSION

In this paper an adaptive control algorithm has been designed for controlling relative position dynamics of a leader and follower spacecraft. The Lyapunov type design adaptive controller law was able to estimate the parameters and the disturbances caused by solar radiation pressure. This facilitates tracking of the reference trajectories with global asymptotic convergence. The use of the Magnetospheric Multiscale Mission spacecraft mission specifications for numerical simulations validates the claim that this controller also works for highly eccentric orbits. Correction of initial conditions reduces the secular growth as shown in the obtained results. This also helps to minimize fuel consumption over time.

## REFERENCES

- [1] D. Scharf, F. Hadaegh, and S. Ploen, "A Survey of Spacecraft Formation Flying Guidance and Control (Part 1): Guidance," in *American Control Conference, 2003. Proceedings of the 2003*, vol. 2, Jun. 2003, pp. 1733–1739.
- [2] H. Schaub and J. L. Junkins, *Analytical Mechanics of Space Systems (2nd Edition)*. Reston, VA, USA: American Institute of Aeronautics and Astronautics, 2009. [Online]. Available: <http://site.ebrary.com/lib/alltitles/docDetail.action?docID=10516789>
- [3] S. S. Vaddi, S. Vaddali, and T. K. Alfriend, "Formation Flying: Accommodating Nonlinearity and Eccentric Perturbations," *Journal of Guidance, Control and Dynamics*, vol. 26, no. 2, 2003.
- [4] F. L. Markley, *Fundamentals of spacecraft attitude determination and control* / by F. Landis Markley, John L. Crassidis., ser. Space technology library ;. Springer,, 2014.
- [5] J. Fontdecaba Baig, G. Metris, P. Gamet, and P. Exertier, *Solar Radiation Pressure Effects on Very High-Eccentric Formation Flying*. [Online]. Available: <http://tdl.libra.titech.ac.jp/journaldocs/recordID/article.bib-01/ZR000000660241>
- [6] H. Wong, H. Pan, M. de Queiroz, and V. Kapila, "Adaptive learning control for spacecraft formation flying," vol. 2. IEEE, 2001, pp. 1089–1094. [Online]. Available: <http://ieeexplore.ieee.org/lpdocs/epic03/wrapper.htm?arnumber=981030>
- [7] J.-J. E. Slotine, W. Li, *Applied Nonlinear Control*. Englewood Cliffs, N.J: Prentice Hall, 1991.
- [8] D. M. Dawson, J. Hu, and T. C. Burg, *Nonlinear Control of Electric Machinery*, 1st ed. New York, NY, USA: Marcel Dekker, Inc., 1998.
- [9] S. P. Hughes, "Orbit Design for Phase I and II of the Magnetospheric Multiscale Mission." [Online]. Available: <http://ntrs.nasa.gov/archive/nasa/casi.ntrs.nasa.gov/20040082062.pdf>